POLITECNICO
MILANO 1863

RE.PUBLIC@POLIMI
Research Publications at Politecnico di Milano

Post-Print

This is the accepted version of:

F. Piscaglia, A. Montorfano, A. Onorati
A Scale Adaptive Filtering Technique for Turbulence Modeling of Unsteady Flows in IC Engines
SAE International Journal of Engines, Vol. 8, N. 2, 2015, p. 426-436
doi:10.4271/2015-01-0395

The final publication is available at https://doi.org/10.4271/2015-01-0395

Access to the published version may require subscription.

When citing this work, cite the original published paper.

Permanent link to this version
http://hdl.handle.net/11311/978504

2015-01-0395

A Scale Adaptive Filtering Technique for Turbulence Modeling of Unsteady Flows in IC Engines

F. Piscaglia, A. Montorfano, A. Onorati
Dipartimento di Energia, Politecnico di Milano, Italy

Copyright © SAE International

Abstract

Swirling flows are very dominant in applied technical problems, especially in IC engines, and their prediction requires rather sophisticated modeling. An adaptive low-pass filtering procedure for the modeled turbulent length and time scales is derived and applied to Menter' original $k-\omega$ SST turbulence model. The modeled length and time scales are compared to what can potentially be resolved by the computational grid and time step. If the modeled scales are larger than the resolvable scales, the resolvable scales will replace the modeled scales in the formulation of the eddy viscosity; therefore, the filtering technique helps the turbulence model to adapt in accordance with the mesh resolution and the scales to capture. The novel turbulence model presented in this work will be called *Dynamic Length Scale Resolution Model* (DLRM), because of its capability to dynamically adapt its behavior according to the grid resolution and to consequently switch from modeling to resolving the turbulent length scales. Validation has been carried out both on a strongly swirling flow through a sudden expansion and on a simple IC engine geometry with one axial central valve; the model seems able to capture unsteady effects and to produce accurate time-averaged results (especially if compared to its standard RANS formulation) and looks particularly suitable when used with grids where turbulence would not be sufficiently resolved for an accurate LES.

Introduction

There are many interesting strategies for unsteady turbulence modeling: Spalart [1] gave an overview and discussion about the advantages and limitations of many of these when applied to general problems. For industrial simulations of IC engines, unsteady RANS (Reynolds averaged Navier-Stokes) equations are established as a standard tool: the complete turbulence behavior is enclosed within appropriate turbulence model which takes into account all turbulence scales, from the largest eddies to the Kolmogorov scale. Turbulent length and time scales are estimated by dimensional considerations, and model transport equations are solved on reasonably coarse grids, that make this approach relatively cheap in terms of computational cost. Despite RANS is able to give a reasonable approximation of the wall shear stress, it is quite well known that the excessive predicted viscous behavior very often damps out the unsteady motion and the flow unsteadiness, because it overestimates the modeled turbulent length and time scales. Also, despite the uniqueness of a solution to the three-dimensional Navier-Stokes equations has yet to be mathematically proven [2], it is generally accepted that the solution is completely determined by the initial and boundary conditions: hence, unsteady RANS cannot account for randomness or independent events in the flow and it is characterized by simulation results that are perfectly repeatable, if constant boundary conditions (and the same computer) are used for the unsteady computation. In Large-Eddy Simulation (LES), the turbulent length scale is related to the computational grid and to the turbulent time scale from the resolved flow without additional equations; as a result, the approach is potentially more accurate and it is able to provide the intrinsic unsteady character of the flow. For this reason, Large-Eddy Simulation has gained popularity and success; on the other hand, as the Reynolds numbers of most engineering flows are usually very large, LES of wall bounded flows very seldom represents an option for full scale industrial simulations, because the computational cost of LES scales near the walls is similar to Direct Numerical Simulation (DNS). In many LES conducted for wall-bounded flows, wall modeling based on logarithmic profile or other theoretical models are used to avoid the high resolution near the walls, so that the computational cost of LES for modeling the free-shear flows is only weakly dependent on the Reynolds number ($\sim Re^{0.4}$). In complex flows, such as in internal combustion engines, the validity of these theoretical models for LES at the walls is questionable and most of the times it does not improve the quality of the results. A very detailed overview about the use, the advantages and the limits of LES when applied to IC engines is discussed in [3]. Since the required grid resolution needs to be extremely high, LES simulation may become very expensive. Hybrid models are all based on the same idea to represent a link between RANS and LES, since they use the best of both worlds: they resolve the turbulence where possible and they model it elsewhere. As a consequence, they try to keep

computational efficiency of RANS and the potential of LES to resolve large turbulent structures, even on coarser grids and with high Reynolds number. In the recent years, several hybrid LES/RANS methods have been proposed in the literature: examples are Detached Eddy Simulation (DES), Limited Numerical Scales (LNSs), hybrid LES-RANS, or second generation unsteady RANS models, including partially averaged NavierStokes (PANS) and scale-adaptive simulation (SAS). A recent application of PANS to IC engine simulation has been shown in [4]. There is obviously the need in IC engines simulation for a turbulence model that can distinguish between what can be resolved and what cannot, at the same time as it produces an accurate estimate of the wall shear stress. Very Large Eddy Simulation (VLES) is another kind of hybrid method which starts to expand as a promising compromise for simulation of industrial flow problems with reasonable computational time and costs. In VLES large turbulence structures are resolved by an unsteady simulation and the minor structures are modeled with an adequate turbulence model. Compared to the LES and similarly to the other hybrid models, the main difference is that with VLES a smaller part of the turbulence spectrum is resolved and the influence of a larger part of the spectrum has to be expressed with the model. In VLES models, the additional requirement is an appropriate filtering technique which distinguishes between resolved and modeled part of the turbulence spectrum. The filtering procedure provides the adaptive characteristic of the VLES models, enabling them to be applied for the whole range of turbulence modeling approaches from the RANS to the DNS; also, it limits the influence of the statistical turbulence model on the unsteady mean flow field.

A VLES model, sometimes also called Variable Resolution (VR) approach, to predict stochastic flows in internal combustion engines is presented. The filtering approach used may be considered converse to the filtering approach that is used in LES. Instead of solving the filtered equations to avoid the computation of small scales, the modeled length and time scales are filtered in order to suppress their negative influence on the unsteady flow field. This approach has been originally developed by Willems [5] and is similar to other approach of Speziale [6, 7] and Fasel [8], because the filter is applied directly to the Reynolds stress tensor and the turbulence model is left unchanged. Similarly to [9], the functional form of the filter is derived from the relation between filtered and non-filtered time scales. In this work, a novel formulation of the functional form of the filter function, including time resolution in the criteria to maintain phase coherence, is proposed and it is applied to compressible flows. The modeled length and time scales are compared with what it can be resolved by the computational grid and time step. If the modeled scales are larger than the resolvable scales, resolvable scales will replace the modeled scales in the formulation of the eddy viscosity. To distinguish between large- and small-scale turbulence, the upper limit of the length scales of non-resolved turbulence is made proportional to the local grid spacing or the product of the local velocity magnitude and the time step of the simulation; there is no lower limit because the mean non-resolved turbulent length scale may be much smaller than the local grid spacing, especially near the walls. This allows for a much coarser grid resolution than in LES; also, the filter will allow large-scale unsteady structures in the flow, and the model will still produce a wall shear stress comparable to what is produced by the standard RANS model. The filtering technique has been applied to a compressible formulation of the $k-\omega$ SST model [10] including the optional sink term for rough walls [11]. Model validation has been performed against experimental measurements on a strongly swirling flow through a sudden expansion [12] and on a flow around a poppet valve [13].

Turbulence Modeling

The compressible formulation of the $k-\omega$ SST model [10] including the optional sink term for rough walls [11] has been used as the basic turbulence model in this work. The main idea behind this choice is to retain the robust and accurate formulation of the RANS model in the near wall regions and in zones of the freestream region where the mesh resolution is not sufficiently high for the direct solution of the main turbulent scales. The model is a two-equation eddy viscosity model, and it is coupled to the averaged Navier-Stokes equations by the eddy-viscosity assumption:

$$-\tau_{ij} = 2\,\mu_t S_{ij} - \frac{2}{3}\rho k \delta_{ij} \tag{1}$$

where τ_{ij} is the viscous stress tensor and S_{ij} is the strain rate tensor, defined as:

$$S_{ij} = \frac{1}{2}\left(\frac{\partial u_i}{\partial x_j} + \frac{\partial u_j}{\partial x_i}\right) \tag{2}$$

The Boussinesq assumption introduces the concept of a turbulent eddy viscosity, μ_t and it is particularly suitable when the influence of turbulence on the mean flow is dominated by a mixing process. The eddy viscosity has the same dimension as the viscosity of the fluid and is assumed to be proportional to a function of the local turbulent length and time scales:

$$\mu_t \sim L_t^2/T_t \tag{3}$$

The turbulent length and time scales are unknown local properties of the turbulent flow and must be modeled. If the modeled turbulent kinetic energy k and specific dissipation rate ω are solved, a measure of the turbulent length and time scales can be estimated.

Derivation of the Filter Function

A low-pass filtering operation is applied to the turbulence model in order to allow the existence of resolvable turbulent scales in the solution of the flow field. Similarly to [9], the form of the filter function is derived from a dimensional analysis and the filter is applied to the turbulent length and time scales, rather than to the turbulent kinetic energy [5]. As it will later discussed, this allows to apply the approach

to any URANS model with minor modifications. The local modeled turbulent length scale can be directly evaluated by the turbulent kinetic energy and dissipation, as follows:

$$L_t \sim k^{1/2}/\omega \tag{4}$$

$$T_t \sim 1/\omega \tag{5}$$

In the approach presented in this work, the filtering operation is based on the comparison between the modeled and the resolved turbulent length scales. The upper limit of the modeled turbulent length scale corresponds exactly to the lower limit of the resolved turbulent length scales. The largest length scale that needs to be a part of the eddy viscosity formulation is:

$$\ell_t = \min\{L_t, \Delta_f\} \tag{6}$$

where Δ_f is evaluated by comparing a function of the local flow velocity $\mathbf{U}$ and an equivalent LES filter size Δ_{eq}:

$$\Delta_f = \max(\alpha|\mathbf{U}|\delta t,\ \Delta_{\mathrm{eq}}) \tag{7}$$

In Eq. (7), the product $\alpha|\mathbf{U}|\delta t$ is a measure of the shortest distance over which a fluid particle can be traced in an unsteady computation and the maximum length scale that needs to be a part of the eddy viscosity formulation. In this sense, the computational timestep influences the lower limit for the resolved time scale and includes the implicit relationship between space and time in the filtering operation. Introducing the maximum flow Courant-Friedrichs-Lewy (CFL) number:

$$\mathrm{CFL}_{\mathsf{max}} = \frac{\mathbf{U}_{\mathsf{max}}\ \delta t}{\delta x_{\mathsf{min}}} \tag{8}$$

the time integration step is usually limited to:

$$\delta t \leq \frac{\mathrm{CFL}_{\mathrm{max}}\ \delta x_{\mathsf{min}}}{|\mathbf{U}_{\mathsf{max}}|} \tag{9}$$

where $\mathrm{CFL}_{\mathrm{max}}$ is usually chosen on the basis of the numerical method and of the level of unsteadiness of the problem.

Being the local CFL number defined on cell *i*:

$$\mathrm{CFL}_i = \frac{|\mathbf{U_i}|\,\delta t}{\delta x_i} \tag{10}$$

the criterion (9) ensures that for each cell the local CFL number CFL_i is lower than the maximum CFL:

$$\beta = \frac{\mathrm{CFL}_i}{\mathrm{CFL}} \leq 1 \tag{11}$$

In general, there is no way to mathematically distinguish between turbulence and unsteadiness. For this reason, it is very difficult to estimate the minimum length scale that the turbulence model is able to capture, since it depends both on the spatial resolution and on the temporal correlation between timesteps, which is strictly related to the CFL used by the numerical solver. A conservative way of thinking would lead to the conclusion that for each computational cell the smallest turbulent length scale that can be captured by the turbulence model is $(|\mathbf{U}|\,\delta t)_{\mathsf{MAX}}$

$$\begin{aligned} |\mathbf{U}|\,\delta t|_{\mathrm{MAX}} &= \mathrm{CFL}\cdot\delta x \\ &= \frac{\mathrm{CFL}_i}{\beta}\ \delta x \\ &= \alpha\ \mathrm{CFL}_i\ \delta x \\ &= \alpha\ |\mathbf{U}|\delta t \end{aligned} \tag{12}$$

where

$$\alpha = \frac{1}{\beta} = \frac{\mathrm{CFL}}{\mathrm{CFL}_i} \tag{13}$$

In [9], numerical experiments suggested that the optimum multiplier α to the product $|\mathbf{U}|\,\delta t$ should be 3 in order to properly resolve the turbulent structures. In the present paper, the coefficient α is dynamically calculated by the model from the local and the overall CFL number, which varies in time and space; this is done to correlate the temporal scales of the vortexes and the spatial resolution of the grid in the filter operation and it is particularly important in engine flows, where cell size and flow conditions significantly vary between the near valve region and the other regions of the mesh. A dynamic procedure for run-time calculation of the integral length scale allows for a more correct estimation of the minimum integral length scale that can be locally captured by the model. In Eq. (7), the (estimated) upper limit of the dissipation range scales is compared to the length of the resolved scales through the Length Scale Resolution (LSR) parameter [14]. LSR provides a relationship between the actual resolved energy level and the corresponding lower limit of the inertial sub-range and it is defined as:

$$LSR = \frac{\Delta}{\ell_{di}} \tag{14}$$

where Δ is the local filter size and ℓ_{di} is the lower limit of the inertial sub-range [15]:

$$\ell_{di} \approx 60\eta \tag{15}$$

and η is the Kolmogorov scale:

$$\eta = \nu^{3/4}\varepsilon^{-1/4} \tag{16}$$

Where the LSR value is equal to 1 all the turbulent scales up to the dissipation range are resolved. From the definition of Eq. (14), the evaluation of the actual resolved energy level is directly linked to the local filter size; in this way the adopted mesh size is related to the local energy resolution all over the computational domain. In [16], it was found that

$$\mathrm{LSR} \leq 5 \tag{17}$$

is the upper limit to guarantee a reasonable resolution is space for LES at an affordable computational cost. From Eq. (17) and (14), it follows that the maximum equivalent filter width Δ_{eq} to use in Eq. (7) is:

$$\Delta_{\mathrm{eq}} \leq \mathrm{LSR}\cdot\ell_{di} \tag{18}$$

The upper limit on the modeled length and time scales ℓ_t can also be defined in terms of the filtered (non-resolved) variables:

$$\ell_t \sim \hat{k}^{1/2}/\hat{\omega} \tag{19}$$

$$t_t \sim 1/\hat{\omega} \tag{20}$$

The specific dissipation rate ω is related to the dissipation rate ε by the relation:

$$\omega = \frac{\varepsilon}{\beta^* \, k} \tag{21}$$

where β^*=0.09. The filtered specific dissipation can be written as

$$\hat{\omega} = \frac{\hat{\varepsilon}}{\beta^* \, \hat{k}} \tag{22}$$

The dissipation rate is never resolved in anything cheaper than a DNS, hence

$$\hat{\varepsilon} = \varepsilon \tag{23}$$

and from Eq. (22) and (23) it follows:

$$\hat{\omega} = \frac{\omega \, k}{\hat{k}} \tag{24}$$

and from Eqs. (4), (19) and (22) an expression for the filtered turbulent kinetic energy can be found:

$$\hat{k} = g(\ell_t, L_t) \, k \tag{25}$$

where the equality follows from the assumption that the constants of proportionality in Eq. (4) and (19) are equal. The filter function results to be defined as:

$$g \equiv (\ell_t / L_t)^{2/3} \tag{26}$$

in which ℓ_t is computed from Eq. (6) and the modeled turbulent scale L_t is calculated as:

$$L_t \simeq \frac{k^{1/2}}{\beta^* \, \omega} \tag{27}$$

In regions where turbulence cannot be resolved, i.e. where $L_t < \Delta_f$ in Eq. (6), the filter function is equal to unity and in Eq. (25) $\hat{k} = k$. However, there is no need to compute the filtered turbulent variables explicitly. A filtered eddy viscosity can be constructed directly from the non-resolvable turbulent length and time scales:

$$\hat{\mu_t} \sim \ell_t^2 / t_t \tag{28}$$

It follows from Eqs. (19), (20), (24) and (25) that

$$\hat{\mu_t} = g^2 \, \rho \frac{k}{\omega} \tag{29}$$

where the equality must hold in order to recover the original (non-filtered) eddy viscosity formulation, $\mu_t = \rho \, k/\omega$, in regions where the filter is inactive. Note that the only modification to the original eddy viscosity formulation is the factor g^2, i.e., the square of the filter function.
The filter function can be derived and applied using any two-equation turbulence model: it will always have the same functional form reported in Eq. (26) and it will always appear as squared when used in the formulation of the eddy viscosity; also, it has an explicit grid dependence in the eddy viscosity formulation through the parameter l_t in Eq. (26) when $\Delta_f < L_t$ in Eq. (6).

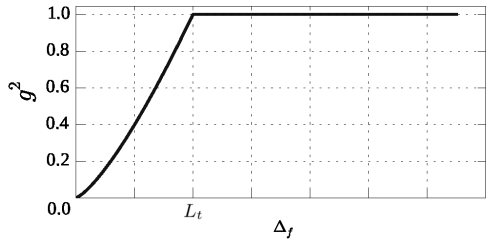

Figure 1: The filter function $g^2(\Delta_f)$ is clipped to 1 as Δ_f is equal to the integral length of the modeled scales L_t and it tends to zero with a minimum as the grid size tends to the fine grid limit.

The definition of Eq. (26) is thought to allow the filter function to go naturally to zero as the grid spacing tends to zero and as the grid size tends to the fine grid limit:

$$\lim_{\Delta_f \to 0} g^2 = 0 \tag{30}$$

Also the derivative of g^2 with respect to the filter width:

$$\frac{\partial \left(g^2\right)}{\partial \Delta_f} = \frac{4}{3} \left(\frac{\Delta_f}{L_t} \right)^{1/3} \tag{31}$$

must tend to zero as $\Delta f \to 0$:

$$\left. \frac{\partial \left(g^2\right)}{\partial \Delta_f} \right|_{\Delta_f \to 0} \to 0 \tag{32}$$

Eq. (31) justifies the choice of applying the filter not only to the kinetic energy k as in [5], but to turbulent scales as well. If the filter was applied only to the turbulent kinetic energy, the square of the filter function $g(\ell_t, L_t)$ in Eq. (29) would vanish and the filter would not have the proper behavior in the fine grid limit, since Eq. (32) would not tend to zero. It must be also noted that the above conclusion holds as long as k and ω do not explicitly depend upon the local grid spacing. Actually, as the eddy viscosity is limited by the filter, there will also be less production of modeled turbulent kinetic energy k and specific dissipation rate, ω. This is natural, because the resolved turbulent kinetic energy and specific dissipation should increase. In Fig. 1 an example of the filter function g^2 is shown. The filter function is clipped to 1 if Δ_f is greater than the integral length of the modeled scales L_t. Finally, the second derivative of the curve near the fine grid limit must be positive, to ensure that in that region small variations of the grid size corresponds to high variations of the resolved scales.

The described model will be called *Dynamic Length Scale Resolution Model* (DLRM), because of its capability to dynamically adapt its behavior according to the grid resolution and to consequently switch from modeling to resolving the turbulent length scales.

Test Cases and Computational Setup

The Dynamic Length Scale Resolution Model has been validated on two different test cases, where experimental data were available:

- A swirling flow through a sudden expansion, whose measurement were published in [12].

- A simplified IC engine configuration, consisting of a circular pipe with a sudden expansion from d = 34 mm to D = 120 mm, with a single axis-centered poppet valve is positioned across the expansion with a fixed lift of 10 mm, to originate a circular jet that expands inside the larger cylinder.

A second-order backward differencing scheme was used for discretizing the temporal derivatives, whereas momentum convection was performed with the Linear-Upwind Stabilized Transport (LUST) scheme, a low-dissipation method specifically developed for LES [17]. For the remaining differential terms, pure second-order differencing schemes were used, with the exception of energy, for which an upwind-biased method was employed for stability. The pressure-velocity coupling was solved using a compressible solver based on the PIMPLE (merged PISO-SIMPLE) algorithm, that has been extended by the authors to work with non-conformal grids [18]. For each case, predictions of the DLRM have been compared with the standard formulation of k-ω SST and of the wall-adapting local eddy viscosity (WALE) model on the same computational grids (where turbulence may not be sufficiently resolved for an accurate LES), in order to compare the capability to predict the unsteady effects and to produce accurate time-averaged results. The computational tool used for the simulations is the open-source finite-volume CFD software OpenFOAM®, that was already extended by the authors with sgs models, boundary conditions, pre- and post-processing applications to perform simulation of turbulent flows with moving boundaries [19, 20, 21, 22, 23, 24].

Swirling flow in a abrupt expansion

A swirling flow through a sudden expansion has been investigated and experimental results from [12] have been used for validation. In the experiments, the swirl number

$$\mathrm{S} = \frac{\int_0^R V_\theta V_z r^2 dr}{R\int_0^R V_z^2 r dr} \tag{33}$$

was approximately 0.6 based on the inlet radius, R=D/2; V_θ and V_z in Eq. (33) denote the time-averaged tangential and axial velocities, respectively. The Reynolds number based on the inlet diameter D and the bulk velocity at the inlet was Re=30000. The axial inlet duct had a diameter of 0.0508 m; its length was 31 diameters and the sudden expansion was located 15 diameters downstream of the swirl generator. Experiments were performed with an incompressible flow (water); swirl was generated by supplying a variable portion of the flow through tangential slots. Both axial and tangential components of mean velocity and rms turbulence levels were measured by Laser Doppler Anemometry (LDA) on a dense grid of points lying in a horizontal plane through the tube centerline. Included in the grid measurement stations were two upstream locations at X/D=-2 and X/D=-0.5. The complete distribution of the measurement stations is shown in Fig. 2.

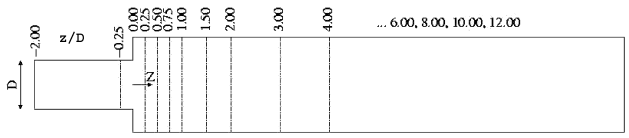

Figure 2: Probe locations in the experimental test rig [12].

In the simulations, two different block-structured grids have been used, with a resolution that is typical of in-cylinder flow calculations: a first grid (that will be labeled as “coarse”) had about 1.5 Million cells, while a “fine” grid was made of about 4 Million cells. The two grids were mainly differing in the resolution of the area near the abrupt expansion, where more turbulent structures need to be captured. Cell centers normal to the wall were placed at $y^+ \sim 2$ in both grids; hence, the coarser grid had larger grid stretching in the wall-normal direction, especially in the near-wall region downstream of the sudden expansion. Also, the coarse grid had an axial resolution that was definitely lower downstream of the abrupt expansion. An incompressible formulation of the solver and of the turbulence model were used; despite in IC engines flows are highly compressible, the aim of the early stage of this work was to validate the theory

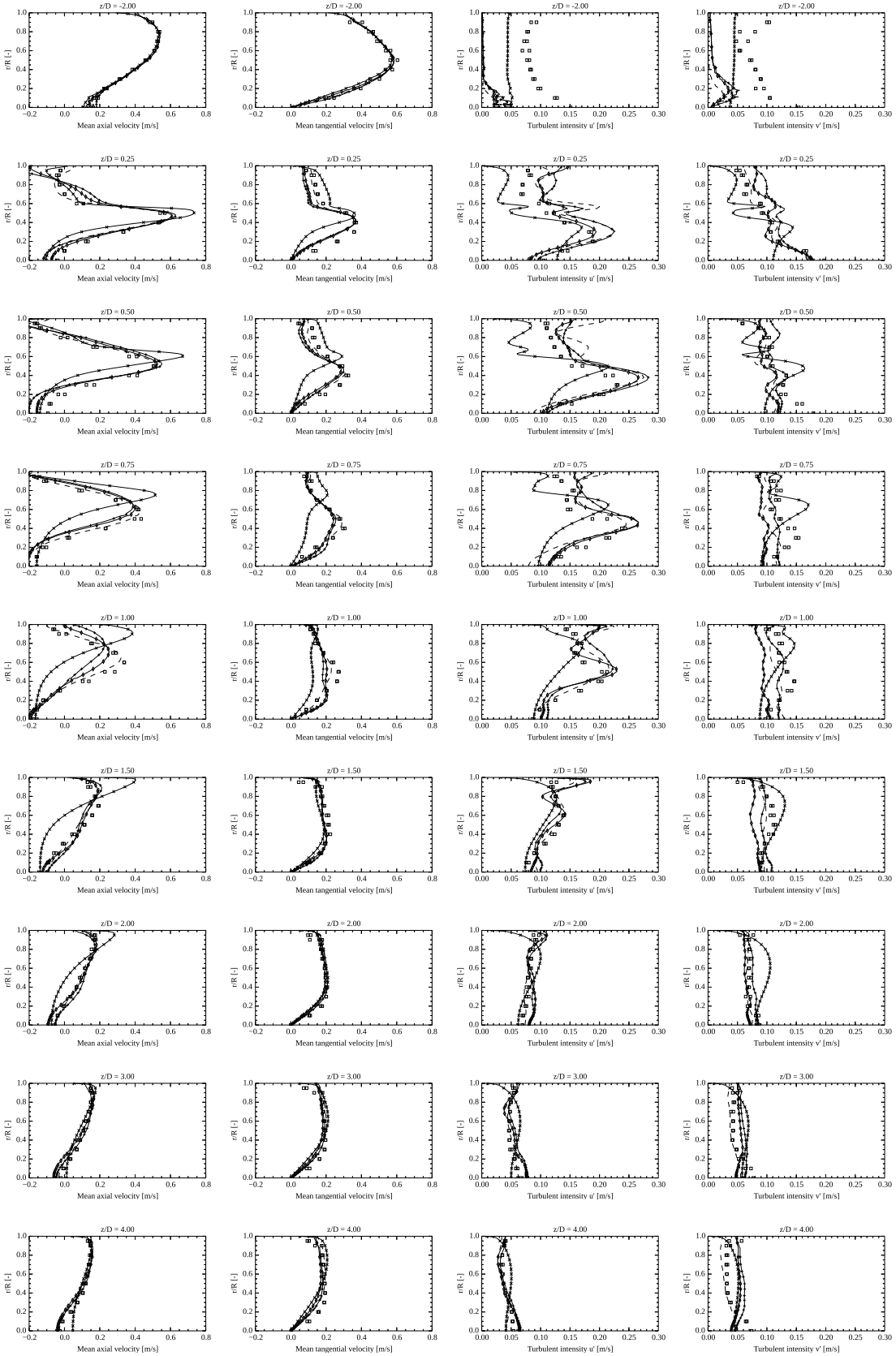

Figure 3: Velocity profiles and rms turbulence levels at different locations: a) mean axial velocity; b) mean tangential velocity; c) axial RMS fluctuations; d) tangential RMS fluctuations. Legend: □ experiments; $-\diamond-$ DLRM (coarse grid); **– –** DLRM (fine grid); $-+-$ WALE (coarse grid); $-\times-$ $k\omega$ SST (coarse grid).

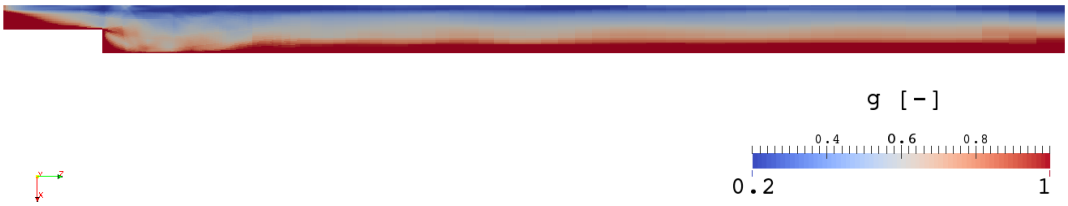

Figure 4: Contour plot of the filter function along the middle section of the geometry studied (time=20 mean flow residence times, coarse grid). The square of the filter function g in the DLRM model is bounded between 0 (DNS, theoretically) and 1 (pure RANS). Pure RANS modeling is used at the walls, where grid resolution is obviously too low for solving turbulent scales of the flow.

of the filtering approach, which is independent by the nature of the flow. Spline curves based on the measured data were used as inlet boundary condition for mean velocities, while constant inlet turbulent intensity was set to 10% on the basis of the levels of axial and tangential Reynolds normal stresses measured in [12]. However, since the swirl level in the present experiment was high enough for a fast transition to turbulence, adding unsteadiness at the steady inlet boundary condition would have been superfluous, as evidenced by the results shown by Fig. 3. Also, since the DLRM model (as any RANS-based filtered model) is not very sensible to the values of the turbulent quantities at the inlet boundary, LES boundary conditions for synthetic turbulence generation [20, 23] were not needed. At the outlet boundary, a homogeneous Neumann boundary condition was used for velocity and temperature, while pressure level was set to ambient; a no-slip condition was used for the velocity at the walls, where the turbulent kinetic energy vanishes. Time-averaged profiles of the monitored quantities have been calculated over 20 mean flow residence times and circumferentially averaged in space. The evolution of the axial and tangential velocity distributions and the predicted rms turbulence levels are shown in Fig. 3 for each z/D available from the measurements. As evidenced, the aim of the DLRM is to allow large-scale unsteady structures in the resolved flow field and to give accurate time-averaged results on a typical RANS grid. In order to see what results can be obtained from a LES on the same grids, a simulation using the WALE sgs model [25] on the grid labelled as “coarse” was performed. Results of Fig. 3 show that DLRM model behaves much better than $k-\omega$ SST all over the domain; the RANS k-ω-SST model has been applied only to the coarse mesh, where grid convergence was satisfied. It is important to notice that since the mean velocity of this case is not particularly high, LSR is often lower that 5 around the abrupt expansion: for this reason, WALE model is able to sufficiently resolve most of the energy-containing turbulent structures in that region, while it does not provide good predictions for z/D$>$1.5, where grid size is too coarse for LES (almost 1 cm along the axial direction, LSR is higher than the threshold). At z/D=-2, quantities at the first computational cell near the inlet boundary are reported. As expected, the profiles of turbulence intensity reflects the behavior of the models adopted: with a pure RANS turbulence model, turbulent intensity is almost constant over the section of the channel, since the model transports the turbulent kinetic energy that is set at the inlet. As the DLRM model is used, the value of the turbulent viscosity in the first computational cell near the boundary is calculated on the basis of the grid refinement: turbulent viscosity results to be lower than the modeled one, as confirmed by the theory [26]. For the same reason, turbulent viscosity calculated by pure LES modeling (WALE) on the same cells results to be also lower when compared to RANS. Fig. 3 also evidences that DLRM improves the predictions of the pure $k-\omega$ SST in the recirculation region, since the original formulation of $k-\omega$ SST is quite insensitive to rotation [26] and damps out unsteady fluctuations during the simulation. Similarly to the filtering procedures [9], DLRM removes the limitations of the $k-\omega$ SST model, while retaining good near wall characteristics. Finally, the contour plot of the time-averaged value of the filter function (Fig. 4) shows that even the coarse grid is sufficiently fine to allow for the direct resolution of most of the scales of interests for the case studied: for this reason, both WALE and DLRM are able to provide good predictions of the average quantities. Finally, DLRM is able to provide reliable predictions of the turbulence intensities u’ and v’ (Fig. 3) also for $\mathrm{z/D} > 2$ and near the walls, where the grid resolution is not high enough for the direct resolution of the turbulent scales (Fig. 4), since it combines the best features of RANS and LES models.

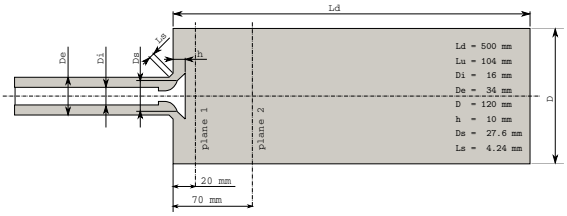

Figure 5: simplified engine geometry [13] used for validation.

Flow around a poppet valve

The second case analyzed is a simplified IC engine configuration (Fig. 5) consisting of a circular pipe where a single axis-centered poppet valve is positioned with a fixed lift of 10 mm, to originate a circular jet that expands inside the cylinder. The cylinder has an outlet open end and the flow is driven by the difference of total pressure between the inlet and the outlet boundary. Air enters the smaller pipe with a mean Reynolds number of about 30000, which corresponds to a bulk velocity of 65 m/s. The flow inside the smaller annular duct is similar to a circular pipe flow; however, in the studied case this region was of minor interest since most

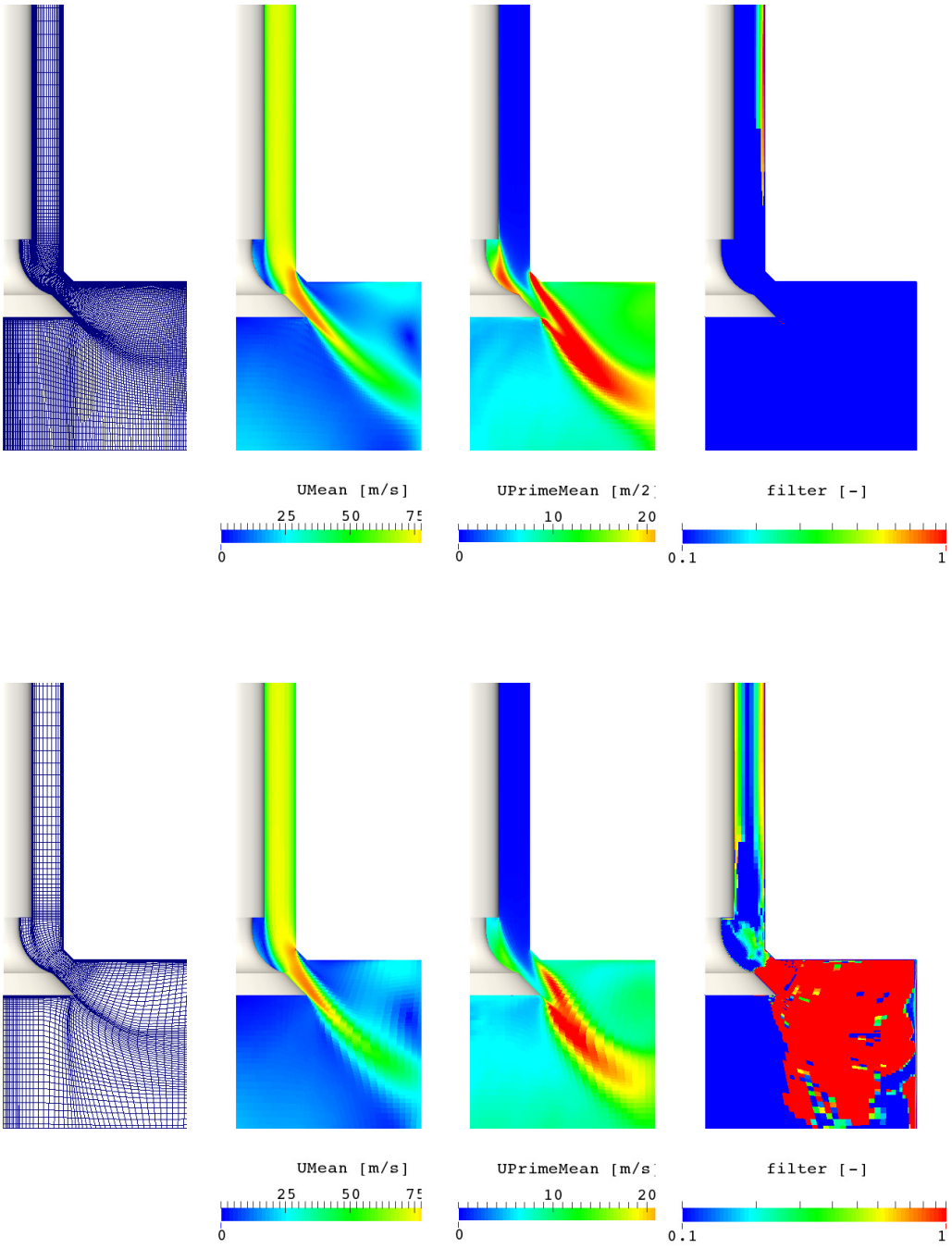

Figure 6: DLRM predictions on two diffent grids: 700k cells ("coarse" grid, first row); 5.3 M ("fine" grid, second row). DLRM is able to smoothly handle the transition from RANS to LES by the blending function g^2, as the local grid resolution changes: this is confirmed by the snapshots of the flow field, that do no show any discontinuity. Space averaging has been applied for the plotted (time-averaged) quantities along the azimuthal direction. Only for the filter function, the color scale used is logarithmic.

of the turbulence production takes place at the shear layer between the circular jet and the cylinder flow that is, initially, at rest. The mesh structure, the flow features and filter function calculated by DLRM are reported in Fig. 6. Contour plots show that highest velocities are located where the jet-like flow extends into the cylinder region. As the intake flow extends beyond the near valve region, flow direction changes at the cylinder wall, creating a clockwise tumble motion. Two large toroidal recirculation zones originate inside the cylinder: the former is located near the upper wall, the latter is close to the cylinder axis. Although simplified, this configuration can be considered as representative of the main flow types that occur in a real engine during the intake stroke, where a high-speed jet coming from the intake valve enters into the cylinder region and originates large-scale motion of the charge. LDA measurements of the mean flow velocity and of RMS fluctuations (along the radial and tangential directions) were available on two planes

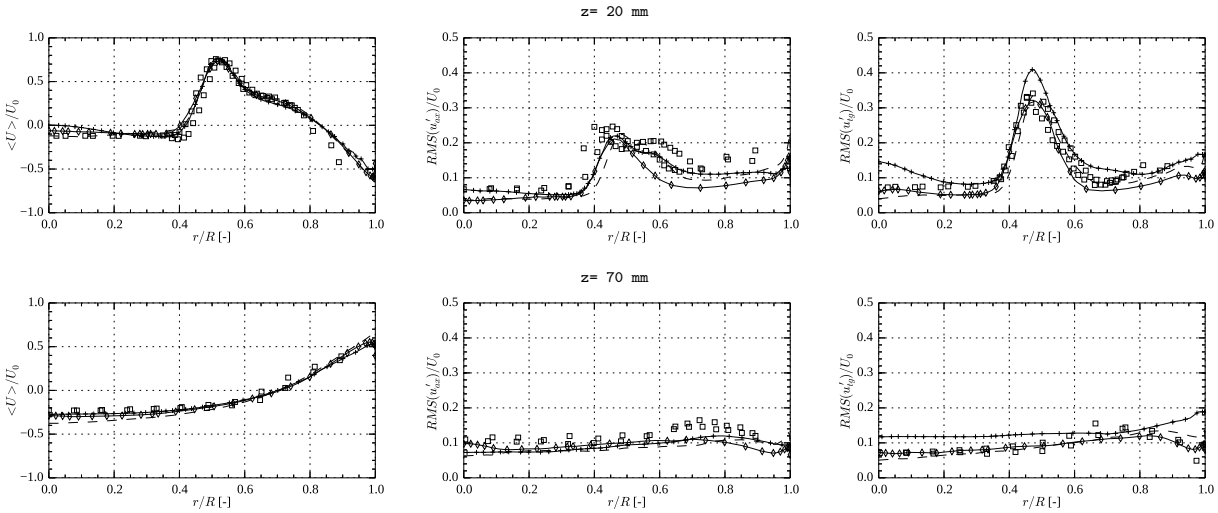

Figure 7: Comparison between predicted velocity profiles and LDA measurements. Plane x=20 mm: a) mean axial velocity b) rms axial fluctuations c) rms tangential fluctuations. Plane x=70 mm: c) mean axial velocity d) rms axial fluctuations e) rms tangential fluctuations. Legend: □ experiments; $-\diamond-$ DLRM (700 k cells); $--$ DLRM (5.3 M cells); $-+-$ WALE (12 M cells).

located at a distance of 20 mm and 70 mm from the cylinder top, respectively. Similar studies on this configuration have already been done in [13] and in [20]. A comparison of simulations carried out with different turbulence models and grids is reported in Fig. 7: the WALE model [25] in its compressible formulation was applied on a grid having a resolution of 12 M cells, that could be considered merely adequate for a proper LES. Predictions with the WALE model [20] were compared with DLRM, that was applied on two different grids, having 700 thousand and 4 million cells respectively. The two grids will be referred in the following to as 'coarse' and 'fine' grid. The resolution of all the grids used was considered fine enough for a complete RANS. For all cases, mesh non-orthogonality was very low (below 40 °), as well as skewness, so the solver convergence was strongly favored; also, grid resolution in the cylinder region was relatively coarse, if compared to the fine cells oriented like the flow used near the valve seat, where most of the turbulence production takes place. The topology of the grid used for DLRM summarizes some considerations coming from early investigations [21], where it has shown the influence of the shear layer instability of the annular jet going from the valve section to the cylinder region on cyclic variability of IC engines: consequently, resolution in the grids used is higher in the jet region in order to let DRLM directly solve the turbulent scales; larger scales in the cylinder are just modeled. In the fine mesh of Fig. 6, non conformal interfaces [27, 28, 24] have been used to unlink the grid resolution between the duct, the jet and the cylinder regions and, therefore, to limit the overall number of cells; the resulting grid was oriented as the jet flow near the valve seat and it is highly refined in the region of the jet flow. The contour plot of the filter function g^2 and of the flow field evidence that where the grid is refined, DLRM resolves more and more turbulent structures. For the coarse mesh, turbulence is mainly modeled by RANS, as a direct (and obvious) consequence of the choice to have only a 700 K cell grid. It is important to note that case setup for DLRM in terms of boundary and initial conditions for turbulence is the same of a RANS simulation. Mean velocity was set at the inlet boundary, while constant inlet turbulent intensity was set to 10% of the mean velocity. The simulations using DLRM (as any other turbulence model based on filtering) is not expected to be sensible to the values of turbulence quantities at the inlet boundary. If the imposed length scale is too large, the filter activates and automatically decreases the production of turbulence via the eddy viscosity, according to Eq. (6). Statistical quantities have been computed by averaging in time over a large number of samples (corresponding to the number of timesteps) during the ten mean flow residence times simulated. The first flow residence time was discarded from the statistical analysis in order to minimize the effect of the initial conditions. Taking advantage of the axisymmetric geometry, space averaging was computed along the azimuthal direction for the time-averaged quantities, in order to reduce the total number of flow-through times to be simulated. Data were sampled with an angular step of 5°; linear interpolation was used to approximate the fields in between cell centers. Both ensemble averaged velocity and rms fluctuations have been extracted from the circumferential-z averaged planes and compared with experimental measurements, as reported in Fig. 7. Profiles have been plotted along the cylinder radius at 20 and 50 mm from the cylinder head, conventionally assumed as z=0. Only the axial component of the mean velocity has been considered for comparison, since no experimental data [13] were available along the other two directions; experiments on rms fluctuations were available instead both along the radial and the axial direction. Both WALE and DLRM provide good predictions of average velocity, since all the grid had a sufficient resolution in the regions studied; when rms fluctuations are considered, then the different characteristics and behavior of the different models is apparent. Predictions by DLRM better agree with experiments than WALE, or they are at least comparable: considering that the grid resolution used with DRLM is only 700 K cells for the 'coarse' mesh, the result can be considered very satisfying. As a higher mesh resolution is used, DLRM progressively resolves a higher amount of turbulent scales, improving the accuracy of the results; grid resolution initially defined by the operator

is the control parameter for the operation of DLRM and this makes the setup particularly simple. Also, the good agreement of DLRM near the walls is favored by the use of RANS wall functions. Experimental data in the near vicinity of the walls (r/R $>$ 0.9) were missing from original LDA measurements, despite this is not so apparent by Fig. 7. Finally, it is important to note that because of the hybrid nature of the DLRM model, a deeper statistical analysis partially loses its significance, because the integral turbulent length scale is not fully resolved everywhere. Hence, detailed flow statistics such as two-point correlations or power spectra would be affected by the application of the filter function, which continuously varies from one cell to another, thus making very difficult to use them to gather clear information about grid convergence; this is the reason why statistical analysis is not reported in the paper. As already mentioned, grids used in this work are too coarse for solve most of the turbulent scales: the aim of the work was to find a model to resolve the scales of interest for an engine simulation on a very coarse grid, rather than trying to resolve all the turbulent scales, as only a complete LES on a very fine grid would be able to describe.

Conclusions

With respect to traditional RANS, predictions of unsteady turbulent flows by DLRM result improved, thanks to the application of an adaptive low-pass filter to the modeled turbulent length and time scales. The novel definition of the filtering function, explicitly though for transient simulations of compressible flows, includes a dependency of the time-resolved scales on the CFL constraint and a criterion based on the Length Scale Resolution parameter, to ensure proper spatial and temporal resolution. The advantages are significant: the computational cost of the model and the case setup, in terms of boundary and initial conditions required are the same of the standard k-ω SST model; the local grid resolution is the parameter that directly influences the way to calculate the turbulent scales. The filter function smoothly controls the transition from cells where turbulence is modeled (RANS) to cells where turbulent scales are directly resolved. With respect to other hybrid models available in the literature, the formulation of the filter used by DLRM allows to avoid discontinuities in the flow field, in particular in the regions where there is transition between different formulations of the turbulent scales. Despite the turbulence model works with any kind of mesh definition (hexahedral, tetrahedral or, in general, polyhedral), the combined use with an accurate compressible solver and high quality mesh [18] favors a very good agreement between simulations and experiments. If compared with WALE, DLRM is computationally more expensive (it is a two equation model, where k and ω are transported); on the other hand, DLRM is able to work with coarse (RANS) grids providing similar results to LES, with a computational effort that is comparable to RANS modeling. If the grid defined by the user is too coarse, DLRM behaves as a $k-\omega$ SST model, hence results must be intended and interpreted as RANS results. The square filter function, which is bounded between 0 and 1, is an indicator of the way to calculate turbulence length scales: a square filter function g=0 would theoretically indicate a direct resolution of the turbulent scales (DNS): this is of course impracticable with the grid resolutions applied in this work (and in general in the field of IC engines), therefore $g = 0$ should be intended as the condition when implicit LES is applied to capture the turbulent scales of interest. The formulation of the filter function g proposed in this work can be easily applied to any RANS turbulence model, making the approach very general.

Acknowledgments

All the simulations presented in this paper were running on Blues, high-performance computing cluster operated by the Laboratory Computing Resource Center (LCRC) at Argonne National Laboratory (ANL). Authors gratefully acknowledge ANL for the computing resources made available within the PETSc-Foam project.

References

[1] Spalart, P.R. Strategies for Turbulence Modelling and Simulations. *Int. J. Heat Fluid Flow*, 21(3):252–263, 2000.

[2] Volker John. On large eddy simulation and variational multiscale methods in the numerical simulation of turbulent incompressible flows. *Applications of Mathematics*, (51):321–353, 2006.

[3] C. J. Rutland. Large-eddy Simulations for Internal Combustion Engines - a Review. *Int. J. Eng. Res.*, (12):421–451, 2011.

[4] B. Basara. Computation of IC-engine-type flows by an extended Partially Averaged Navier-Stokes model with a novel scale supplying equation. International Multidimensional Engine Modeling User's Group Meeting 2014, The Detroit Downtown Courtyard by Marriott Hotel, Detroit, MI (USA), April 7th, 2014.

[5] W. Willems. *PhD thesis*. PhD thesis, Institut fur Technische Mechanik, RWTH Aachen, 1996.

[6] C.G. Speziale. Turbulence Modeling for Time-Dependent RANS and VLES: A Review. *AIAA Journal*, 36:173–184, 1998.

[7] C.G. Speziale. A Combined Large-Eddy Simulation and Time-Dependent RANS Capability for High-Speed Compressible Flows. *J. Sci. Comput.*, 13(3):253–274, 1998.

[8] H.F. Fasel, J. Seidel, and S. Wernz. A Methodology for Simulations of Complex Turbulent Flows. *J. Fluids Eng.*, 124:933–942, 2002.

[9] W. Gyllenram and H. Nilsson. Design and Validation of a Scale-Adaptive Filtering Technique for LRN Turbulence Modeling of Unsteady Flow. *Journal of Fluids Engineering*, 130:051401, 2008.

[10] F. R. Menter. Two-equation eddy-viscosity turbulence models for engineering applications. *AIAA Journal*, 32(8):1598–1605, 1994.

[11] A. Hellsten. Some Improvements in Menters k-Omega-SST turbulence model. In AIAA, editor, *29th AIAA Fluid Dynamics Conference*, 1998.

[12] P.A. Dellenback, D.E. Metzger, and G.P. Neitzel. Measurements in turbulent swirling flow through an abrupt axisymmetric expansion. *AIAA Journal*, 26(6):669–681, 1988.

[13] L. Thobois, G. Rymer, T. Soulères, and T. Poinsot. Large-eddy simulation in IC engine geometries. Sae Paper n. 2004-01-1854, SAE world Congress & exhibition, 2004.

[14] F. Brusiani, C. Forte, and G. Bianchi. Assessment of a Numerical Methodology for Large Eddy Simulation of ICE Wall Bounded Non-Reactive Flows. In *SAE Technical Paper 2007-01-4145*, 2007.

[15] S.B. Pope. *Turbulent Flows*. Cambridge University Press, 2000.

[16] F. Brusiani and G. M. Bianchi. Basic numerical assessments to perform a quasi-complete LES toward IC-engine applications. In *Proceedings of the ASME 2010 International Mechanical Engineering Congress & Exposition*, IMECE2010, Vancouver, British Columbia, Canada, November, 12-18 2010.

[17] H. Weller. Controlling the computational modes of the arbitrarily structured C grid. *Monthly Weather Review*, 140:3220–3234, 2012.

[18] A. Montorfano, F. Piscaglia, and A Onorati. An Extension of the Dynamic Mesh Handling with Topological Changes for LES of ICE in OpenFOAM. In *SAE Technical Paper 2015-01-0384*. SAE International, 04 2015.

[19] F. Piscaglia, A. Montorfano, A. Onorati, and F. Brusiani. Boundary Conditions and SGS Models for LES of Wall-Bounded Separated Flows: An Application to Engine-Like Geometries. *Oil Gas Sci. Technol. - Rev. IFP Energies nouvelles*, 69(1):11–27, 2014. Link.

[20] F. Piscaglia, A. Montorfano, and A. Onorati. Towards the LES Simulation of IC Engines with Parallel Topologically Changing Meshes. *SAE paper 2013-01-1096, SAE Int. J. Engines*, 6(2):926–940, 2013. Link.

[21] A. Montorfano, F. Piscaglia, and A. Onorati. A LES Study on the Evolution of Turbulent Structures in Moving Engine Geometries by an Open-Source CFD Code. *SAE Technical Paper 2014-01-1147*, 2014.

[22] F. Piscaglia, A. Montorfano, and A. Onorati. Development of a Non-Reflecting Boundary Condition for Multidimensional Nonlinear Duct Acoustic Computation. *Journal of Sound and Vibration*, 332(4):922–935, 2013. Link

[23] F. Piscaglia, A. Montorfano, and A. Onorati. Improving the Simulation of the Acoustic Performance of Complex Silencers for ICE by a Multi-Dimensional Non-Linear Approach. *SAE Int. J. Engines*, 2(5):633–648, 2012.

[24] F. Piscaglia, A. Montorfano, and A. Onorati. Development of Fully-Automatic Parallel Algorithms for Mesh Handling in the OpenFOAM-2.2.x Technology. *SAE Technical Paper 2013-24-0027*, 2013. Link.

[25] F. Nicoud and F. Ducros. Subgrid-scale stress modelling based on the square of the velocity gradient tensor. *Flow, Turbulence and Combustion*, 62:183–200, 1999.

[26] D. C. Wilcox. *Turbulence Modeling for CFD*. DCW Industries Inc., 2006.

[27] F. Piscaglia, A. Montorfano, and A. Onorati. Development of Fully-Automatic Parallel Algorithms for Mesh Handling in the OpenFOAM-2.2.x Technology. In *International Multidimensional Engine Modeling User's Group Meeting 2013, The Detroit Downtown Courtyard by Marriott Hotel, Detroit, MI (USA)*, April 14th 2013. Link.

[28] F. Piscaglia, A. Montorfano, and A. Onorati. A Moving Mesh Strategy to Perform Adaptive Large Eddy Simulation of IC Engines in OpenFOAM. In *International Multidimensional Engine Modeling User's Group Meeting 2014, The Detroit Downtown Courtyard by Marriott Hotel, Detroit, MI (USA)*, April 7th 2014. Link.

[29]